

Nonlinear Radiation Pressure and Stochasticity in Ultraintense Laser Fields

Joel E. Moore

Massachusetts Institute of Technology, Cambridge, MA 02139

The radiation force on a single electron in an ultraintense plane wave ($a = eE/mc\omega \sim 1$) is calculated and shown to be proportional to a^4 in the high- a limit, with a weak dependence on the wave polarization. The cyclotron motion of an electron in a constant magnetic field and an ultraintense plane wave is numerically found to be quasiperiodic even in the high- a limit if the magnetic field is not too strong, as suggested by previous analytical work. A strong magnetic field causes highly chaotic electron motion and the boundary of the highly chaotic region of parameter space is determined numerically. Applications to experiments and astrophysics are briefly discussed.

It has been known for many years that qualitative changes occur in the behavior of an electron moving in an electromagnetic plane wave when the dimensionless strength $a = eE/mc\omega$ is of order unity. Recent advances in laser pulse compression and amplification [1] have made it possible to attain such ultraintense waves in the laboratory and led to new investigations of their properties. One important effect is that an electron moving in an ultraintense electromagnetic plane wave and also subjected to slowly varying “background” fields behaves approximately like a particle of enhanced mass moving only in the background fields. The fast motion in the wave can be rigorously averaged over if the background fields are sufficiently weak and the plane wave is not so strong that pair creation effects become significant.

This Letter considers what happens to the enhanced-mass approximation when two effects ignored in its derivation are included. The first effect considered is nonlinear scattering of the incident wave, which is shown to give rise to a radiation force on the quasiparticle which is quadratic in the incident power for strong fields. Because of the enhanced-mass effect, the resulting acceleration for strong fields scales as (power) $^{3/2}$. This radiation force depends on the polarization of the incident wave (not unexpected since the total radiated power is known to depend on polarization [2]) but this dependence drops out in the low- and high-field limits. The second effect considered is the destruction of the enhanced-mass behavior as the strength of the background fields is increased to violate the field-strength condition $eB_{\text{back}}/mc\omega_{\text{wave}} \ll 1$ necessary for the enhanced-mass derivation. This suggests that the field-strength condition is a real physical limit on the enhanced-mass description. Both effects are expected to be significant in astrophysical situations, and the first effect may well be visible in laboratory experiments with ultraintense laser pulses.

Classical calculations are valid for high a as long as the discrete photon energy $\hbar\omega \ll mc^2$ and the amplitude for QED processes such as e^+e^- pair creation is small ($eE\hbar/mc \ll mc^2$) [3]. The classical high- a regime includes a number of existing and proposed accelerator designs, such as the plasma wakefield and beat-wave accelerators [4]. Lasers used in the National Ignition Facility and similar inertial fusion projects have $a \sim 1$ so

strong-field effects are significant, and current experimental tests of strong-field QED should see a quantum analogue of the nonlinear radiation force calculated here. Many astrophysical problems also involve high- a radiation sources [5].

The classical averaging to find the drift motion of the electron guiding-center in the enhanced-mass regime [6] gives the same mass enhancement factor γ_0 as appears in the calculation of the Dirac propagator for an electron dressed by a plane wave [7]. In quantum-mechanical terms the enhanced mass occurs because the electron has absorbed a wave photons more than it has radiated, on average. The resulting off-mass-shell electron has charge e and enhanced mass $m\gamma_0 = m\sqrt{1 + e^2\langle A_\mu A^\mu \rangle/m^2c^4}$. Here A is the vector potential and $\langle \rangle$ denotes averaging over the wave phase. For a linearly polarized monochromatic wave $\gamma_0 = \sqrt{1 + a^2/2}$. The enhanced mass appears classically because the electron is relativistic over its fast orbit in the intense plane wave, so its inertia to other applied forces is increased.

The motion of an electron in a plane wave of arbitrary intensity is integrable both classically and within the Dirac equation. This occurs because a third conserved quantity $\gamma - p_x$ exists in addition to the two transverse generalized momenta. Here γ is the electron Lorentz factor and p_x is the component of electron momentum along the wave axis. Including radiative effects or adding additional fields generally violates this conservation. The result of the scattering of the wave by the electron is a force on the electron along the wave axis, which has the form $F = 2e^4\langle E^2 \rangle/3m^2c^4$ for weak plane waves. In the high- a regime the electron radiates much more strongly ($\propto a^4$ rather than a^2 in the low- a limit) and radiates high harmonics of the wave frequency [2]. Some care must be taken to calculate the radiation force for a strong plane wave correctly, since the electron can have different γ and hence different inertia at different times in its motion in the plane wave.

We consider monochromatic linearly and circularly polarized waves as examples and then generalize to polychromatic and arbitrarily polarized incident waves. The motion in a circularly polarized wave is simple: in the “drift frame” where the electron has zero average velocity, its motion is a circle in the plane perpendicular

ular to the wave axis, with constant energy $mc^2\gamma = mc^2\sqrt{1 + (eE_0/mc\omega)^2}$. For a linearly polarized wave along $\hat{\mathbf{x}}$ with $\mathbf{E} = E_0 \cos \eta \hat{\mathbf{y}}$, $\mathbf{B} = E_0 \cos \eta \hat{\mathbf{z}}$, $\eta = \omega(t - x/c)$, the motion is a figure-eight in the xy plane with energy $mc^2\gamma = mc^2(\gamma_0 - a^2 \cos 2\eta/4\gamma_0)$. The radiation reaction force from the scattered photons causes the drift velocity (the velocity of the drift frame) to change in time. The drift velocity component along the wave axis changes for an applied force \mathbf{F} (in addition to the force from the wave) according to [6]

$$\frac{dv_d^x}{dt} = \frac{F_x}{m\gamma} - \frac{F_y v_y}{mc\gamma_0} - \frac{F_z v_z}{mc\gamma_0}. \quad (1)$$

The instantaneous radiated power is given by

$$\begin{aligned} P &= \frac{2e^4}{3m^2c^3} ((\mathbf{E} + \frac{\mathbf{v}}{c} \times \mathbf{B})^2 - (\mathbf{E} \cdot \frac{\mathbf{v}}{c})^2) \gamma^2 \\ &= \frac{2e^4}{3m^2c^3} \gamma^2 E^2 (1 - v_x/c)^2 = \frac{2e^4}{3m^2c^3} \gamma_0^2 E^2. \end{aligned} \quad (2)$$

The radiation reaction force on the electron is $\mathbf{R} = -\mathbf{v}P/c^2$ and the total force on the electron is $\mathbf{F} = \mathbf{R} + P\hat{\mathbf{x}}/c$, where the second term reflects the fact that if photons are radiated isotropically the electron still picks up momentum since photon momentum is being removed from the incident wave. The drift acceleration is then

$$\begin{aligned} \frac{dv_d^x}{dt} &= \frac{2e^4 E^2}{3m^3 c^4} \left(\frac{\gamma_0^2}{\gamma} + (v_y/c)^2 \gamma_0 + (v_z/c)^2 \gamma_0 \right) \\ \Rightarrow \frac{dv_d^x}{d\eta} &= \frac{2e^4 E^2}{3m^3 c^4 \omega} \frac{\gamma^2 + \gamma_0^2 - 1 - (\gamma v_x)^2}{\gamma} \\ &= \frac{2e^4 E^2}{3m^3 c^4 \omega} \left(2\gamma_0 - \frac{1}{\gamma} \right). \end{aligned} \quad (3)$$

The average over phase η can now be carried out—the first term is trivial, but the second term depends on the wave polarization. Naïvely summing the radiation force and then dividing by the averaged mass γ_0 gives γ_0 rather than $2\gamma_0 - \langle \frac{1}{\gamma} \rangle$. Thus the correct acceleration is twice as large in the high- a limit. For a circularly polarized wave γ is constant and the acceleration is $(2e^4 E_0^2 / 3m^3 c^4)(2\gamma_0 - 1/\gamma_0)$. For linear polarization the average is

$$A_{\text{linear}} = \frac{e^4 E_0^2}{3m^3 c^4} \left[2\gamma_0 + \frac{4\gamma_0}{a^2} - \frac{1 + 4\gamma_0^2/a^2}{\sqrt{\gamma_0^2 - a^4/16\gamma_0^2}} \right]. \quad (4)$$

For linearly and circularly polarized waves of equal intensity, $A_{\text{linear}} \leq A_{\text{circular}}$ with equality in the low- a and high- a limits. The radiation force can be defined as the required constant force to balance the above acceleration: $F_{\text{rad}} = m\gamma_0 A_{\text{rad}} = (2e^4/3mc^3)(2\gamma_0^2 \langle E^2 \rangle - \gamma_0 \langle E^2/\gamma \rangle)$. As an example, for $a = 1$ the radiation force is $1.901F_0$ for linear polarization and $2F_0$ for circular polarization (with the same intensity), with $F_0 = 2e^4 \langle E^2 \rangle / 3m^2 c^4$ the radiation force from the nonrelativistic expression. For $\lambda = 1 \mu\text{m}$ the force F_0 is 190 eV/cm . For $a = 10, \lambda = 1 \mu\text{m}$, the corresponding figures are $F_{\text{linear}} = 100.55F_0$, $F_{\text{circular}} = 101F_0$, $F_0 = 19 \text{ keV/cm}$.

For $a > 1$ the radiation force is dominated by the term $\propto 2\gamma_0^2 \langle E^2 \rangle$. The force from this term can be calculated directly from the power spectrum. For a blackbody distribution of temperature T and total intensity I , the result is $\gamma_0^2 = 1 + (10\pi\hbar^2 e^2 I / m^2 c^3 k_B^2 T^2)$, and for I/T^2 sufficiently large that the second term in γ_0^2 dominates, $F \approx 160\pi^2 e^6 I^2 \hbar^2 / m^4 c^8 k_B^2 T^2$.

It is useful to clarify the differences between the radiation force and the (longitudinal) ponderomotive force, which also acts along the axis of the wave. The longitudinal ponderomotive force, observed in recent experiments [8], acts only when the wave's envelope is rising or falling, and arises from the conservation of the quantity $\gamma - p_x$. (There are also transverse ponderomotive forces in real beams arising from the finite spot size; these have a different character and are not discussed here.) The net effect of the ponderomotive force from a laser pulse is a displacement of the electron in the direction of the pulse without any change in velocity. The radiation force does not conserve $\gamma - p_x$ and always acts in the forward direction, unlike the ponderomotive force, which is directed forward when the wave is rising and backward when the wave is falling. Treating an electron in a plane wave as an enhanced-mass particle acted upon by ponderomotive and radiation forces gives a nearly complete description of single-particle behavior in the classical regime.

Now we turn to consider the second effect discussed in the opening: the modifications to the enhanced-mass picture when strong constant electromagnetic fields are added to the plane wave. In the following the wave will be taken to have constant amplitude and ponderomotive and radiation forces will be neglected. For definiteness consider adding a constant magnetic field $\mathbf{B} = B\hat{\mathbf{z}}$ to a linearly polarized wave $A_y(\xi)$ traveling in the $\hat{\mathbf{x}}$ direction. Then p_z is constant and we take $p_z = 0$ so that the electron motion is confined to the xy plane. This configuration of fields was chosen because it is the simplest which shows the wide variety of possible behavior. For small wave strength $a_w = eE/mc\omega$ the motion can be analyzed perturbatively because the equations of motion are nearly linear [9]. Special-relativistic effects act as small nonlinear perturbations which tend to move electrons away from resonance as their energy varies.

When a_w is of order unity, the equations are strongly nonlinear and new phenomena appear. However, the motion is still simple for $a_w > 1$ as long as the applied magnetic field is not too strong. In the derivation of the equations for the motion of the guiding-center, it was necessary to assume $a_b = eB/mc\omega = \omega_c/\omega \ll 1$, i.e., the electron is far from resonance. Fig. 1 shows a typical trajectory when the enhanced-mass picture is applicable ($a_w = 1.5$, $a_b = 0.02$): the electron executes fast oscillations in the wave, while its guiding-center makes a slow orbit in the magnetic field. In this section we study numerically the breakdown of the enhanced-mass picture when $\omega_c/\omega \sim 1$. The nonlinearity in the equations of

motion resulting from the electron's relativistic velocity will be shown to destroy integrability over part of phase space. This is in contrast to the previously studied integrable motion when the magnetic field is parallel to the wave axis [10].

With no wave present the gyrocenter of the electron motion $(x_0, y_0) = (x + p_y/eB, y - p_x/eB)$ (with $m = c = 1$) is constant in time. The kinetic energy $E = \gamma$ is also conserved. The energy is no longer conserved when the wave A_y is added because the Hamiltonian is now time-dependent. Within the linear approximation an unlimited amount of energy can be transferred to the electron at resonance ($\omega_c = eB/mc = \omega_{\text{wave}}$). The possibility of resonance makes it somewhat surprising that the electron still has a well-defined gyrocenter when the wave is added. This gyrocenter reduces to the normal gyrocenter when the wave strength is zero and is exactly constant for an arbitrarily strong wave. Its coordinates are

$$(K_x, K_y) = \left(x + \frac{p_y + eA_y(\xi)}{eB}, y - \frac{p_x + 1 - \gamma}{eB}\right). \quad (5)$$

The constants of motion in (5) are combinations of the wave-only constants and the magnetic-field-only constants. Such a gyrocenter exists for any direction of the magnetic field $B_0 \hat{\mathbf{b}}$ and any polarization of the wave: $\mathbf{r}_c = \mathbf{r} - (\mathbf{r} \cdot \hat{\mathbf{b}})\hat{\mathbf{b}} - \hat{\mathbf{b}} \times (\mathbf{p} + e\mathbf{A}(\xi) + 1 - \gamma\hat{\mathbf{k}})/eB_0$.

Now consider again the particular case $\hat{\mathbf{k}} \parallel \hat{\mathbf{x}}$, $\mathbf{A} \parallel \hat{\mathbf{y}}$, $\mathbf{B} \parallel \hat{\mathbf{z}}$. Taking $p_z = 0$ confines the motion to the $x - y$ plane so that phase space is five-dimensional (position (x, y) , momentum (p_x, p_y) , and time t). The constants (5) reduce the effective dimension of phase space by two. Choosing particular values $K_x = K_y = 0$ of the constants corresponds to shifting the gyrocenters of all possible trajectories to the origin, removing two translational degrees of freedom. After this shift, p_x and p_y are no longer independent coordinates but rather functions of x and y determined by (5).

The existence of two constants of motion reduces the effective phase space in this particular case from five dimensions to three. Hamiltonian motion in a two-dimensional phase space is always integrable, so that three-dimensional motions such as the driven pendulum and the Chirikov-Taylor problem [11] are the simplest that can exhibit nonintegrable behavior. The equations of motion after a change to the independent variable $\eta = t - x/c$ and introducing dimensionless parameters $a_b = \omega_c/\omega$, $a_w = eE_0/mc\omega$, and a monochromatic wave $A(\eta)$ are ($\omega = m = c = 1$):

$$\begin{aligned} \gamma &= 1 + \frac{a_b^2 y^2 + (a_b x - a_w \sin \eta)^2}{2(1 + a_b y)} \\ \frac{dx}{d\eta} &= \frac{\gamma}{1 + a_b y} - 1, \quad \frac{dy}{d\eta} = \frac{a_b x - a_w \sin \eta}{1 + a_b y}. \end{aligned} \quad (6)$$

These equations are integrated numerically for various values of a_b , a_w , and the initial conditions $x(\eta_0), y(\eta_0)$.

Because the equations of motion (6) are periodic in η , it is convenient to plot the electron's (x, y) coordinates after each period to study the long-time behavior. This gives an area-preserving map of the plane to itself. Fig. 2 shows a typical surface of section obtained in this way. For low values of the electron initial energy, the motion is quasiperiodic and nearly circular, while for large values of the initial energy the motion is chaotic, as demonstrated by numerically calculated Liapunov exponents (Fig. 3). As time increases the largest exponent for trajectories beginning on points A, B, C is decreasing to zero, while for points D, E, F the largest exponent remains positive, indicating that neighboring initial points separate exponentially rapidly [12]. The electron's initial energy affects the character of the motion because a_b can be much larger in the rest frame of an electron than in the lab frame if the electron has a large initial velocity. To eliminate this effect the initial electron drift velocity is fixed at $0.5c$ henceforth.

The enhanced-mass description predicts that the guiding-center of the electron moves in a circle: $(x_{\text{gc}}(t), y_{\text{gc}}(t)) = (x_0 + (v_d/\Omega) \sin \Omega t, y_0 + (v_d/\Omega) \cos \Omega t)$, with $v_d = 0.5c$ and $\Omega = \omega_c/\gamma_0\gamma_d = a_b\omega\sqrt{1 - v_d^2}/\gamma_0$. At the end of each wave period, $x_{\text{gc}}(t)$ and $y_{\text{gc}}(t)$ are compared with the actual location of the guiding-center calculated from (6). As a dimensionless measure of the error we use the normalized sum of squares error over a cyclotron orbit:

$$E_{\text{gc}} = \left(\frac{\Omega}{v_d}\right)^2 \sum_{\omega(t_n - x_n/c) = 2n\pi}^{\Omega t_n < 2\pi} (\mathbf{r}(t) - \mathbf{r}_{\text{gc}}(t))^2. \quad (7)$$

The error is found to be quite small ($E_{\text{gc}} < 0.01$) for all values of a_w studied as long as $a_b < 0.04$. For each value of a_w , E_{gc} increases rapidly to order unity once a_b reaches a certain critical field: as a threshold we define $a_b^{\text{crit}}(a_w)$ as the value of a_b where $E_{\text{gc}} = 0.01$. Consistent with the predictions of the enhanced-mass picture, a_b^{crit} remains nonzero for large a_w (and in fact increases slightly with a_w). Even though high a_w makes the equations (6) quite nonlinear, the motion remains quasiperiodic and nearly circular for $a_b < a_b^{\text{crit}}$.

As a_b increases above a_b^{crit} , eventually the trajectory with initial velocity $0.5c$ becomes chaotic (has a positive Liapunov exponent) at some value a_b^* . For large a_w , above a_b^* the motion is strongly chaotic and the electron energy fluctuates wildly. This differs from nearly linear resonance at small a_w in that no tuning of frequencies is necessary for energy gain and hence energy gain is not limited by relativistic detuning. Fig. 4 shows numerical curves for a_b^{crit} and a_b^* as part of a schematic phase diagram. The dotted line (which was not calculated and is only schematic) separating the quasilinear resonance phase from the strong stochasticity phase can be defined by the destruction of the last invariant torus at large energy, since in three dimensions such a torus bounds the

energy of trajectories contained within it. Rax has previously proposed that the stochastic motion of electrons in *multiple* plane waves may give rise to high-energy cosmic rays [13].

We verified that approximately the same boundary for the guiding-center description applies when the applied wave is a superposition of two or three applied frequencies. It seems natural to conjecture that the guiding-center region in Fig. 4 also describes waves of finite bandwidth and other orientations of the magnetic field (excluding the integrable case $\mathbf{B} \parallel \mathbf{k}$).

The author wishes to thank Deepak Dhar for many helpful conversations. This work was supported by a U.S. Fulbright grant and a fellowship from the Hertz Foundation.

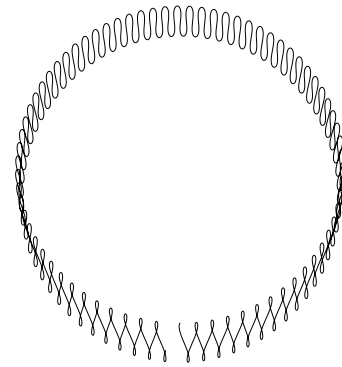


FIG. 1. Typical electron cyclotron motion with $a_w = 1.5$, $a_b = 0.02$, $\mathbf{B} \parallel \hat{\mathbf{z}}$ and $\mathbf{k} \parallel \hat{\mathbf{x}}$.

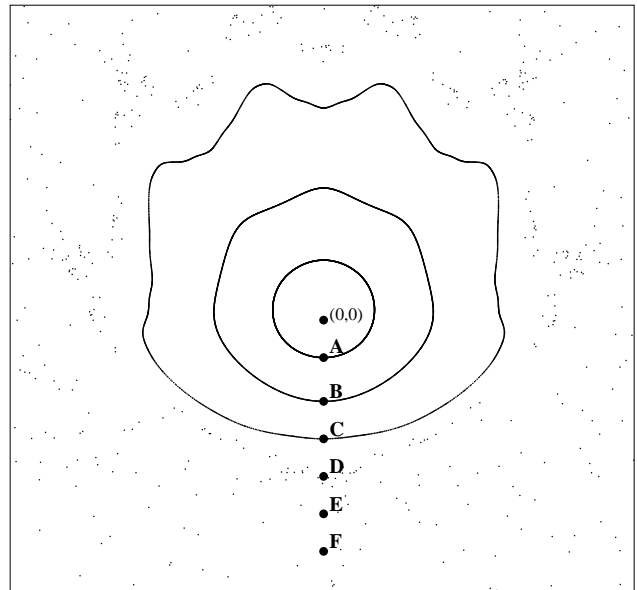


FIG. 2. Surface of section showing trajectories from six different initial conditions with $a_w = 0.1$, $a_b = 0.18$.

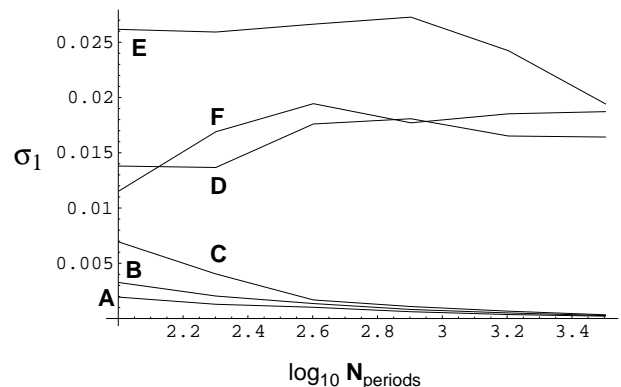


FIG. 3. Numerical largest Liapunov exponent σ_1 calculated at different times for trajectories starting on the six labeled points in Fig. 2.

-
- [1] M. D. Perry and G. Mourou, *Science* **264**, 917 (1994).
 - [2] L. D. Landau and E. M. Lifshitz, *The Classical Theory of Fields*, 4th revised English ed. (Pergamon, London, 1975), §48, 73, 78.
 - [3] F. V. Hartemann and A. K. Kerman, *Phys. Rev. Lett.* **76**, 624 (1996).
 - [4] T. Tajima and J. M. Dawson, *Phys. Rev. Lett.* **43**, 267 (1979); P. Chen and J. M. Dawson, in *Laser Acceleration of Particles*, ed. C. Joshi and T. Katsouleas, AIP Conf. Proc. No. 130 (American Institute of Physics, New York, 1985).
 - [5] F. C. Michel, *Rev. Mod. Phys.* **54**, 1 (1982).
 - [6] J. E. Moore and N. J. Fisch, *Phys. of Plasmas* **1**, 1105 (1994).
 - [7] reviewed in C. Itzykson and J.-B. Zuber, *Quantum Field Theory* (McGraw-Hill, New York, 1980), p. 100.
 - [8] G. Malka and J. L. Miquel, *Phys. Rev. Lett.* **77**, 75 (1996).
 - [9] C. F. F. Karney, *Phys. Fluids* **21**, 1584 (1978).
 - [10] P. C. Clemmow and J. P. Dougherty, *Electrodynamics of Particles and Plasmas* (Addison-Wesley, Reading, MA, 1990), pp. 122-126.
 - [11] B. V. Chirikov, *Phys. Rep.* **52**, 265 (1979).
 - [12] A. J. Lichtenberg and M. A. Leiberman, *Regular and Chaotic Dynamics*, 2nd edition (Springer-Verlag, New York, 1992), p. 298.
 - [13] J.-M. Rax, *Phys. Fluids B* **4**, 3962 (1992).

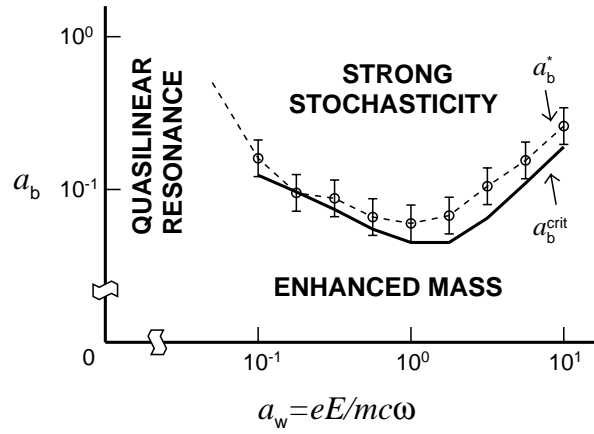


FIG. 4. Numerical values a_b^{crit} and a_b^* for various a_w as part of schematic phase diagram. Error bars are shown for a_b^* because it is difficult to determine precisely when the largest Liapunov exponent becomes positive.